7. ANALYTICAL METHODS

Four surface analysis methods that are often used in the field of catalysis are described in this chapter:

- Electron Spectroscopy for Chemical Analysis (ESCA)
- Auger Electron Spectroscopy (AES)
- Secondary Ion-Mass Spectroscopy (SIMS)
- Scanning Electron Microscopy - Energy Dispersive Spectroscopy (SEM-EDS)

This chapter discusses the fundamentals of each method, their applications, and their limitations.

7.1 ELECTRON SPECTROSCOPY FOR CHEMICAL ANALYSIS (ESCA)

Electron spectroscopy for chemical analysis (ESCA), which is also called x-ray photoelectron spectroscopy (XPS), is used to identify surface atoms and to provide information about the chemical state of these atoms.

ESCA is based on a high resolution analysis of the electrons emitted from the core orbitals of a sample atom upon irradiation by nearly monochromatic x-rays. ESCA gives a unique spectrum for every atom in the periodic table, except hydrogen. If ν is the frequency of the x-ray and E_k is the kinetic energy of the emitted electron, then E_b, the binding energy of the electron at the level from which it was emitted, is obtained according to the energy conservation relation

$$E_b = h\nu - (E_k + C) \qquad (7.1)$$

C is a correction constant that depends on the properties of the particular spectrometer system (11). The binding energy is specific for a given electron in a given element and can serve to identify that element.

Although the ESCA electrons come from the core orbitals, their binding energies are affected by the electronic structure, oxidation state, and bonding of that atom to other atoms on a solid surface. This sensitivity is called a chemical shift and ranges up to about 10 eV for many elements (12). The chemical shifts in ESCA provide additional information about the chemical state of the atom.

ESCA is essentially a surface analysis tool. However, the ESCA electrons emitted from atoms in sublayers 30-60 A deep can have measurable contributions. For solid samples having BET surface areas of 400 m^2/g or above, the difference between "surface" and bulk may be obscured. For solids with a surface area less than 100 m^2/g, this does not seem to be a problem (13).

Currently, there are standard ESCA procedures for handling solid samples prior to and following treatment or reaction. Each laboratory appears to adopt its own specific ESCA procedures. Since ESCA is extremely sensitive to surface contamination, utmost care must be taken in handling samples. Also, the reporting of ESCA results should include detailed descriptions of the equipment and operating procedures. Several examples of using ESCA techniques are given below.

Devices such as those used by Brown (14) allow a close examination of catalytic surfaces as they undergo changes during the course of a reaction (Figure 7-1). Here, the XPS equipment consists of a reaction chamber and an ultrahigh vacuum (UHV) chamber with an x-ray gun and an electron analyzer. The catalyst sample is mounted on a transfer rod, which can move the catalyst to the reaction position or to the analytical position. Brown used this device to study a commercial Co-Mo-Al_2O_3 hydrotreating catalyst under sulfiding and hydrotreating reactions. The device was referred to as being "in situ capable." This may be misleading, since the ESCA was not performed in situ. It was presumably in situ in the sense that the catalyst sample was kept within the reactor-UHV system by the tranfer rod mechanism.

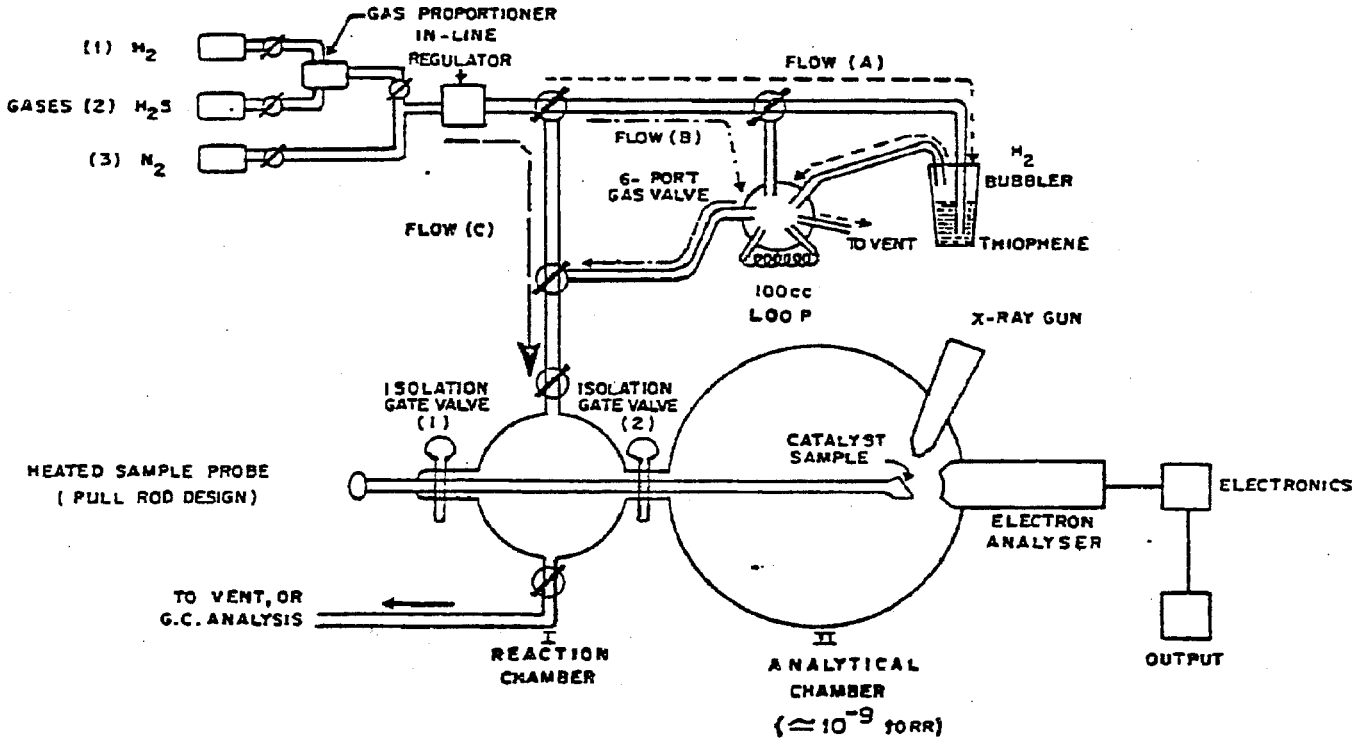

Figure 7-1. Schematic of the Experimental Configuration Used for the Direct Surface Examination of Reacted Catalyst Samples by XPS. Flow (A) (----) is used to load the 100 ml loop with hydrogen gas saturated with thiophene. Flow B (-·-·-·-·) is used to flush the loaded loop of thiophene/H_2 into the reactor. Flow C (- - -) is used to pass H_2, H_2S/H_2, or N_2 directly into the reactor.

Reference: (14)

Bonzel (9) describes an ESCA system with a transfer rod similar to the one used by Brown, but with other analytical capabilites. In addition to XPS, it has an ion sputter gun to clean solid surfaces, an electron gun, a high-resolution electron spectrometer, an Auger electron spectrometer, and a mass spectrometer. This analytical system is described in more detail in Section 7-2.

Multifunctional surface analysis equipment is gaining popularity because of obvious advantages. The analysis of a given sample by the sophisticated methods of this equipment provides evidence leading to an increasingly accurate interpretation of surface phenemena. A commercial unit with Auger electron spectroscopy, secondary ion-mass spectroscopy, ion-scattering spectroscopy, and x-ray photoelectron spectroscopy is now available (14).

7.2 AUGER ELECTRON SPECTROSCOPY (AES)

AES is named after its discoverer, Pierre Auger. It is an electron spectroscopy that is highly sensitive to the top few atomic layers of solid surfaces. Although the theory of AES is fairly involved, the application to most solid surfaces of industrial interest is quite simple.

AES is based on a secondary emission process. Bombardment of a sample atom with a high-energy electron beam (1-10 keV) leads to ionization in one of the inner shells. The atom subsequently rearranges its electron distribution by filling the ionized shell with an electron from a higher-energy orbit or from the valence band. In doing so, the atom releases either a photon (x-ray fluorescence) or an electron, the so-called Auger electron. The energy of the Auger electron is a function only of the emitting atom, and not of the incident beam energy. Measurement of the Auger electron energy therefore allows identification of the emitting atom for all elements of the periodic table except H and He.

AES detects all atoms present in the path of the activating x-ray. For optimal results, gaseous molecules must be excluded from the environment. This means that an ultrahigh vacuum must be used. It also means that AES cannot be used to study the catalytic surface under operating conditions. In situ measurements are

becoming possible using many analytical techniques, including UV, ESR, and SEM. However, there are intrinsic limitations when using AES for in situ applications.

With AES no sample preparation is necessary. Rather, care should be taken to avoid sample contamination.

AES provides spatial resolution to 0.01 mm or ~10μ. Table 7-1 lists other features of AES. Unlike ESCA, AES is not sensitive to the state of the subject atom in chemical bonding, because the chemical shifts are generally not registered by AES.

Table 7-1

AES Features

Sample size	0.1-100 mm
Beam diameter	0.01-0.1 mm
Sampling depth	4-20 A
Sample preparation	none
Signal-to-noise ratio	100-1000
Detection limit	0.01-0.001 monolayer
Detection ability	All elements except H and He
Quantitative analysis	Yes, relative concentration
Elemental peak separation	Very well separated

Reference: (8)

For Fischer-Tropsch catalysis work, numerous AES applications can be cited. Two examples are given below.

Clean sample foils of Rh or Fe were tested in the multifunctional apparatus shown in Figure 7-2 (7). It consisted of a diffusion pump, an ultrahigh vacuum bell jar (1×10^{-9} ton) equipped with a retarding grid, an Auger electron spectroscopy system, a quadrupole gas analyzer, and a 2-keV ion sputter gun. Housed in the bell jar was an isolatable microbatch reactor that operated at elevated temperatures and 1-20 atms while the ultrahigh vacuum was maintained in the bell jar.

The clean metal surfaces were prepared in the ultrahigh vacuum by ion sputtering (Ar^+, 2 keV, 100 μA) at high temperatures (800°C) for 15-20 minutes and then annealing at 700°C for two minutes. Once a clean surface was prepared, the isolation cell was closed and the synthesis gas was introduced while the sample foil was resistively heated to desired temperatures. At any point in the reaction the cell could be evacuated, the sample cooled to room temperature, and the cell opened to the ultrahigh vacuum to allow AES analysis. The pump-down procedure from 6 atm to 5×10^{-8} torr took approximately one minute.

Under Fischer-Tropsch conditions of 300°C, 6 atm, and $H_2/CO = 3$, both the Rh and Fe surfaces produced large amounts of methane, which were accompanied by smaller amounts of higher molecular weight products. Figure 7-3 shows the product distributions.

AES analyses showed that the active metal surfaces (both Rh and Fe) were covered with a monolayer of carbon; no chemisorbed oxygen was detected. Unlike the Rh, the Fe surface did not remain active long. After 120 minutes, the product distribution changed to pure methane and the rate of the reaction decreased markedly. The AES spectra shown in Figure 7-4 describe the carbon buildup on the Fe surface. AES measurements during a post-treatment of the carbon-poisoned Fe foil with a H_2-Ar mixture showed that carbon can be removed as methane.

In a second example of using AES in Fischer-Tropsch catalysis work, CO hydrogenation over polycrystalline Fe foil and single-crystal ^{110}Fe was studied using an experimental system consisting of a stainless steel ultrahigh vacuum

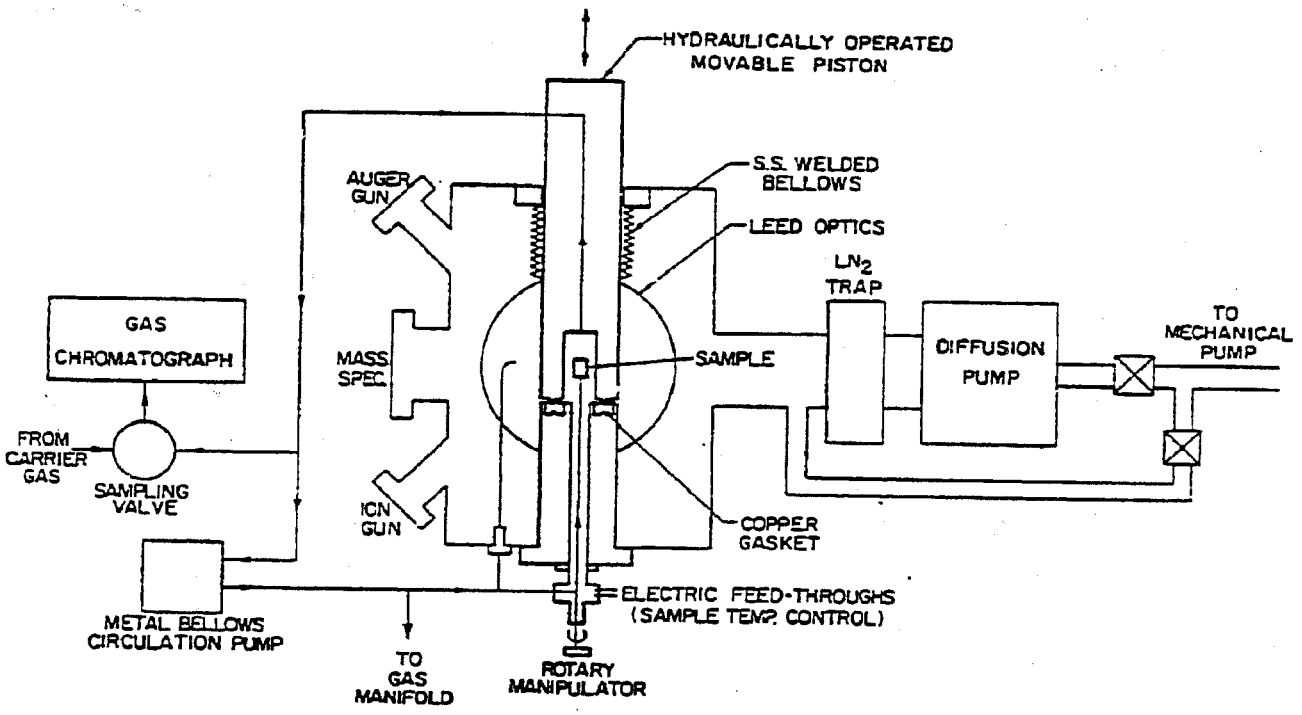

Figure 7-2. Schematic of UHV Surface Analysis System Equipped with Sample Isolation Cell for High-pressure (1-20 atm) Catalytic Studies

Reference: (7)

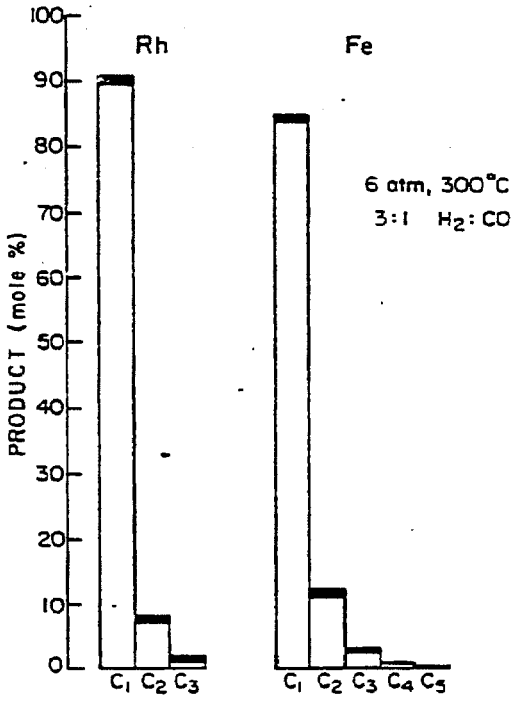

Figure 7-3. Comparison of Product Distributions Obtained over Initially Clean Polycrystalline Iron and Rhodium Foils

Reference: (7)

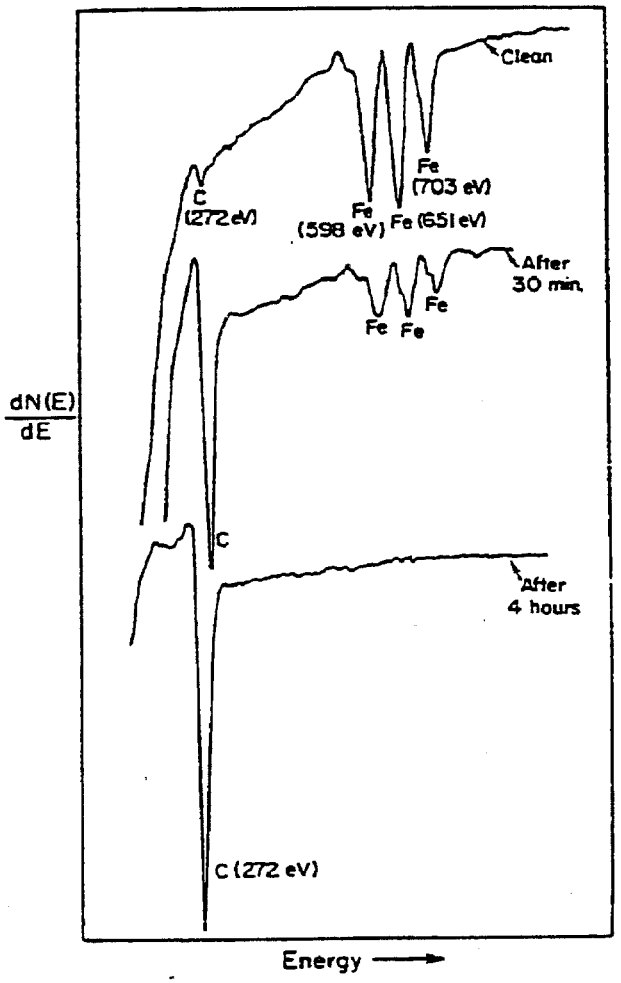

Figure 7-4. Auger Spectra of the Iron Surface before and after 30 min and after 4 h of Reaction. Reaction conditions: 6 atm, 3:1 H_2:CO, 300°C.

Reference: (7)

chamber with an attached microreactor (Figure 7-5). The catalyst sample was attached to a water-cooled transfer rod that could travel along the axis to three positions of different pressure: (a) catalyst loading, (b) reaction (1 atm, <900K), and (c) analytical position (10^{-8} torr, <1400K). The catalyst sample was resistively heated.

The UHV chamber was equipped with an ion sputter gun for surface cleaning, an electron gun, an x-ray source and high-resolution electron spectrometer for Auger electron and x-ray photoelectron spectroscopies, and a quadrupole mass spectrometer for residual gas analysis. The cleaned Fe sample was transferred from the UHV into the reactor where a steady flow of CO/H_2 was already established. As soon as the sample was positioned, the temperature was raised to the desired level. To end the reaction, resistive heating was stopped and a few seconds later, the sample was transferred to the analytical position for AES and/or XPS under UHV. In this fashion, it was possible to continuously monitor the surface species as they changed during the course of the reaction.

Figure 7-6 shows XPS of a carbon (1s) signal at different reaction times for some experimental conditions. For this test, the Fe sample was moved between the reactor and the analytical position for continued XPS monitoring. This figure shows the rapid increase in surface carbon concentration and also a shift in the E_b of the C 1s level from about 283.9 eV to 284.6 eV.

Figure 7-7 shows the AES of three different carbon phases existing on the Fe surface. By comparing the E_b of known carbon forms, three carbon phases were identified. Phase I is due to a CH species that is also detected when C_2H_2 is decomposed on an Fe surface. Phase I may be called the fresh carbon form on the catalytic surface. Phase II is a carbidic carbon layer with bonded hydrogen. The amount of bonded H in this phase is presumably less than in the CH_x layer. This phase is probably the outgrowth of the Phase I carbon. Phase III is graphitic carbon. Peaks labeled A, B, and C provide reference points for identification.

When the Fe surface covered with all three carbon phases was exposed to a hydrogen atmosphere at elevated temperature, Phases I and II disappeared rapidly, leaving behind the Phase III carbon. It was concluded that catalytic surface

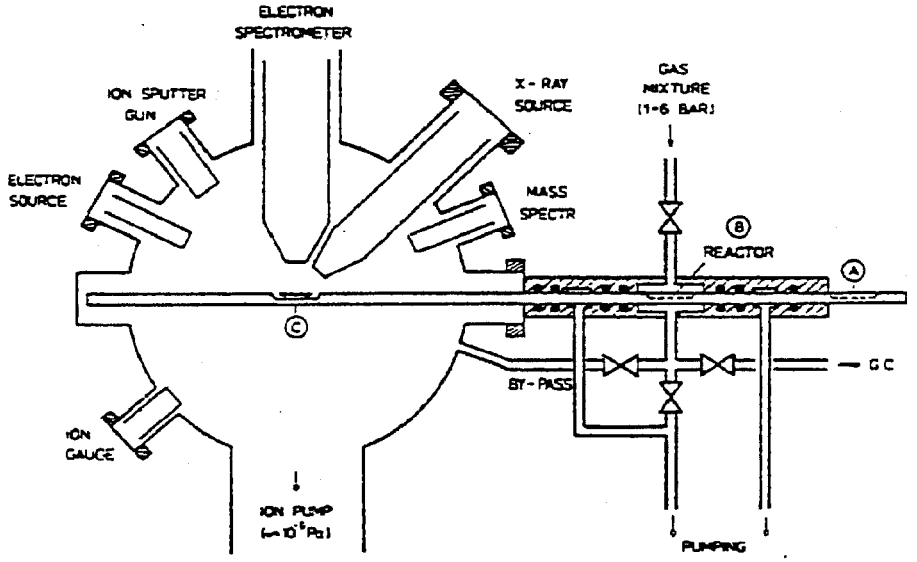

Figure 7-5. Schematic of UHV Apparatus with Attached Sample Transfer System and Microreactor for Catalytic Rate Measurements. The sample, located at the surface analysis position "C" (in the center of the UHV chamber), can be moved by pulling the stainless steel rod to position "B" (reactor for chemical reaction) or position "A" (the atmospheric loading position).

Reference: (9)

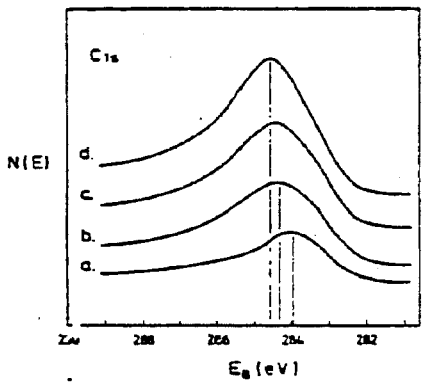

Figure 7-6. Carbon 1s XPS Data after Reaction. CO/H_2 = 1:20, T = 530K, reaction times: (a) 3 sec, (b) 23 sec, (c) 83 sec, and (d) 600 sec. Note shift in maximum.

Reference: (9)

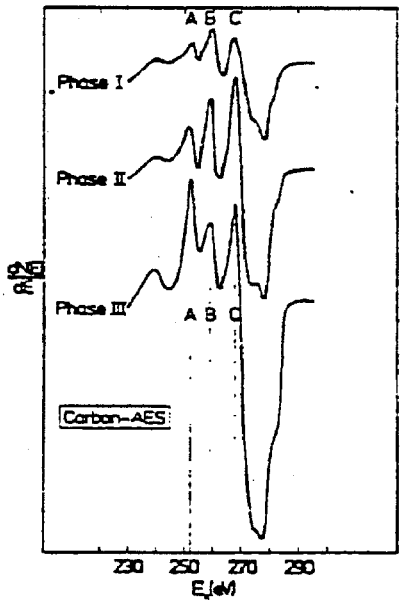

Figure 7-7. Carbon Auger Spectra of the Three Carbonaceous Surface Phases Formed after the CO/H_2 Reaction at 1 Bar and CO/H_2 = 1:20. Reaction conditions: Surface Phase I - T = 565K, t = 15 sec; surface phase II - T = 615K, t = 15 sec; surface phase III - T = 615K, t = 90 min.

Reference: (9)

associated with the Phase I and II carbons is active in Fischer-Tropsch reactions, while Phase III carbon deactivates the catalytic sites.

7.3 SECONDARY ION-MASS SPECTROSCOPY (SIMS)

When energetic ions (primary ions) collide with a solid surface, depending on the kinetic energy of the incident ions, the target material may be ionized and driven away from the solid surface as secondary ions (both positive and negative) which can be detected by mass spectrometry. This is called sputtering--the basis of secondary ion-mass spectrometry (SIMS). Unlike the traditional mass spectrometry that is applicable to vaporizable samples, SIMS can analyze nonvaporizable materials.

SIMS apparatus consists of a stainless steel ultrahigh vacuum chamber equipped with a primary ion generator, a quadrupole mass spectrometer with an energy filter, a sample holder and manipulator, a sample transfer port, and an electron flood gun (36,37). The electron flood gun is needed to compensate, as necessary, for the charges on sample surfaces due to primary-ion bombardment. Figures 7-8 and 7-9 show designs of SIMS apparatus.

Because SIMS is based on sputtering, it is well suited for depth profiling of thin film components. Most SIMS work has involved studying semiconductors, oxides, and metals (36,38).

Bombardment of the target with a beam of high-energy primary ions (such as He^+, Ne^+, Ar^+, Xe^+, and H^+) of 200 to 20,000 eV causes sputtering of secondary atoms, molecules, and clusters in the form of positive, negative, and neutral species. Using electrostatic lenses, the ions are drawn into a mass spectrometer for mass analysis. The successful application of SIMS to chemical structural analysis has been restricted by the lack of information regarding fragmentation of the target molecule and recombination of fragments resulting in so-called clusters. SIMS spectra would reflect all ionic species including the clusters and correct identification of surface species by means of SIMS would be feasible only when the clustering is understood and controlled.

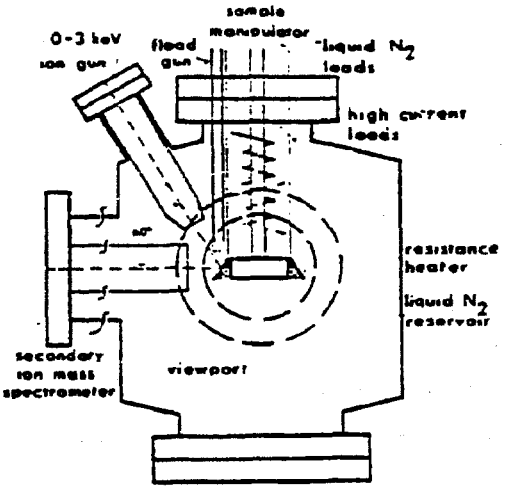

Figure 7-8. Schematic Diagram of the Spectrometer Chamber Showing the SIMS, Sample Carousel, Liquid Nitrogen Cooling System, and Ion Bombardment Gun.

Reference: (37)

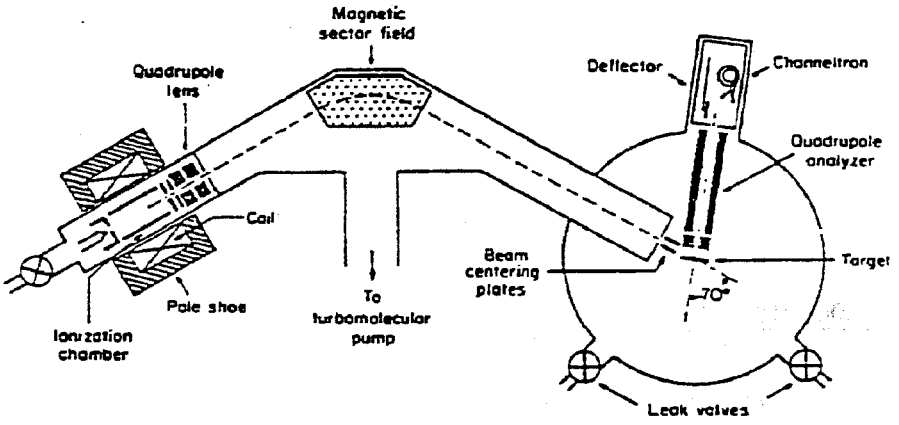

Figure 7-9. Schematic of a SIMS with Mass-selected Primary-Ion Beam

Reference: (36)

SIMS for organic samples is more complex than that for metals and semiconductors. However, there has been substantial progress in experimental techniques, and a new SIMS, called "molecular SIMS," is emerging, with some creative applications already known (34,36,39,40). Molecular SIMS can ionize organic samples without causing them to undergo uncontrolled fragmentation and cluster formation (10, 34). Several ionization techniques are being developed (34), adding versatility to the method.

For catalysis research SIMS can be a powerful tool, but its applications have been fairly limited. With the emergence of molecular SIMS, the potential should be further enhanced. The combination of the traditional solid-state SIMS and molecular SIMS offers the means of investigating the adsorbates as well as the adsorbent in catalysis.

7.4 SCANNING ELECTRON MICROSCOPY AND ENERGY DISPERSIVE SPECTROSCOPY (SEM/EDS)

SEM provides images of surface species with about a 10-nm (point-to-point) resolution (15). By using monochromatic electron beams of short wavelength, SEM can achieve much higher resolution than an optical microscope. Electrons are focused by either electrostatic or electromagnetic lenses. A typical arrangement of these lenses is shown in Figure 7-10. The final lens (objective) controls the focal point of the beam, and the first lens (condenser) controls the size of the beam. With the aid of the scanning coils, electron beams sweep over the surface of the specimen. In scanning mode, electron beams can be stopped and fixed on some surface feature of interest. At this point, the characteristic x-rays emitted by the atoms under the electron bombardment can be analyzed. This x-ray analysis is called energy dispersive spectroscopy (EDS).

The SEM images and chemical identities are obtained by the detectors that collect the secondary and back-scattered electrons and by x-rays that originate from the collision of the scanning (primary) electron beam with the specimen (Figure 7-10). The information carried by these radiations and detector types is listed in Table 7-2.

Table 7-2

Information Carried by Radiation Emitted from Surfaces

Radiation type	Contrast developed mainly from	Use
Secondary electrons	Surface irregularities	To see surface topography
Backscattered electrons	Differences in atomic number	To see alloy constituents and corrosion products
X rays	Different elements	To identify alloy constituents and corrosion products
Auger electrons	Different elements	To identify elements very close to the material surface

Reference: (24)

When imaging is done using the transmitted beam (as compared to the reflected radiation in SEM), the technique is called transmission electron microscopy (TEM). TEM can be operated in scanning mode, which is called scanning transmission electron spectroscopy (STEM). Both TEM and SEM can be operated together with EDS, as can STEM. The resolution of STEM is 0.5-2 nm. SEM and TEM are conducted under a high vacuum that ranges between 10^{-5} and 10^{-7} torr (15).

Sample preparation for electron microscopy is an important part of the analytical procedure. Of this, the sample coating is particularly important as expert judgement is required.

Most nonconducting samples must be coated with a thin layer of a conducting material, usually precious metals or carbon, prior to electron microscopy. This is because a specimen of high resistivity develops static charge under the incident electron beam and may cause a dielectric breakdown in certain regions of the specimen. This leads to variations in the surface potential, giving rise to complex image artifacts (25).

Various thin film techniques are used to coat the sample. Vacuum evaporation and sputtering are frequently used. On an absolutely flat specimen surface, a layer of 0.5-nm-thick carbon forms a continuous coating. A layer ten times as thick is required to form a coating on an irregular surface. Careful attention should be given to the coating method and thickness, because artifacts related to the coating may influence the microscopy analysis. Obviously, each application requires some optimization in terms of coating material, technique, and thickness.

The ability to observe samples at the atomic level is every researcher's wish. To this end, progress is being made both in hardware development and in applications of electron microscopy. Today, a transmission electron microscope equipped with an electron accelerator capable of 1250 kV is said to achieve a maximum resolution of about 1.8 A. This resolution enables observation of heavy metal atoms, but not light ones such as oxygen, nitrogen, and carbon. For light atoms, an ultimate resolution of less than 1 A is required, but important technical breakthroughs are

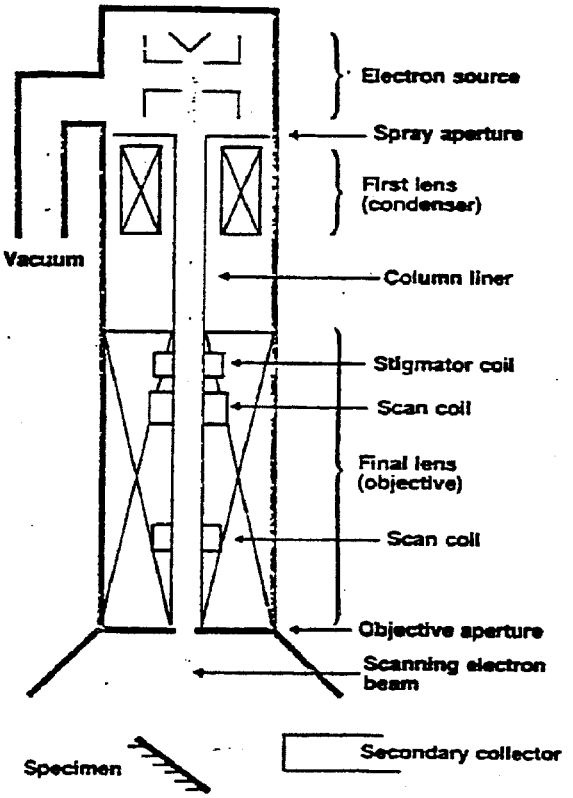

Figure 7-10. SEM Illumination System Showing the Parts of the System that Can Usually Be Controlled by the Operator.

Reference: (24)

needed to achieve this goal. These include a higher accelerating voltage, low-aberration lenses, bright electron sources, a sample stage, and image recording (26).

There are many applications of electron spectroscopy to catalysis research. A particularly fruitful area has been the investigation of strong metal-support interactions (SMSI). This is covered in Section 6. Another noteworthy development is controlled atmosphere electron microscopy (CAEM). CAEM is done with a transmission electron microscope with a specially designed specimen chamber that allows a controlled reaction atmosphere while maintaining the required vacuum in the rest of the system. This arrangement allows in situ observation of heterogeneous reactions at close to the molecular level. In the specimen chamber of CAEM, the sample can be heated to any desired temperature. Furthermore, gaseous reactants can be maintained up to 30 kNm^{-2} (4.5 psia). Under these conditions, the microscope is capable of achieving a resolution of up to 3 nm. This is somewhat lower than a typical transmission electron microscope because of the special design and the presence of gases in the specimen chamber (28).

CAEM images can be continuously monitored and recorded on video tape. The video taping is particularly interesting because it allows the repeated viewing of chemical phenomena at close to the atomic level and because it provides kinetic information on a real-time basis.

Gasification of carbon by metals was studied by Baker of Exxon using CAEM (30). This paper contains useful information pertaining to steam reforming and covers the CAEM of carbon formation, carbon gasification, and catalyst sintering.

For example, when cobalt on silica was exposed to acetylene at 650°C, two types of carbon were observed. One was filamentous carbon, which grows in length according to a sigmoid rate curve, with an initial acceleration period, an intermediate maximum-rate region, and a final deceleration period. The other carbon formed was of the amorphous type. Amorphous carbon forms around supported metal particles and appears to engulf the metal particles, effectively blocking their surfaces to gas adsorption.

Filaments formed from the interaction of supported iron, cobalt, chromium, and nickel with acetylene shared many common characteristics. In all cases, the metal particle was lifted from the support and carried at the growing end of the filament. The width of the filament was governed by the size of the metal particle at its end. Inspection of an active catalyst particle showed that part of its surface was exposed to the gas phase, while for inactive filaments, the catalyst particles were completely covered by carbon. Controlled oxidation of the filaments revealed that they consist of a duplex structure: an inner core of easily oxidizable carbon, surrounded by a skin of more oxidation-resistant material, probably graphite.

Figure 7-11 shows the growth rate of filaments from decomposition of acetylene over iron, nickel, and cobalt. It is clear that the filaments grow fastest (~15 sec.) with nickel, but they do not grow beyond 100 A. The cobalt-catalyzed filament grows longest, about 250 A, and takes about 60 sec. to stop growing.

Baker points out that CAEM can also be used to study catalyst sintering. Sintering is believed to be related to mobility of supported catalyst particles. When iron particles deposited on graphite were heated in various gases, they became mobile on the surface at a definite temperature which was related to the bulk melting point of the particular metal. Table 7-3 lists the mobility temperatures for various metals with a particle size of 100 A. Interestingly, the mobility temperature is very close to the Tammann temperature, which is calculated from the relation: 0.52 bulk temperature in K. The Tammann point is the temperature of onset of mobility of ionic lattice atoms. In a system where there are relatively weak intermediate forces between a particle and its support, one would expect to see particle mobility at the Tammann temperature.

The mobility can be divided into two types:

- Completely random mode, or typical Brownian motion
- Vibrational movement about a fixed point.

The particle displacement rate for silver was obtained at 365°C and is shown in Figure 7-12. As temperature was increased, the curves moved progressively

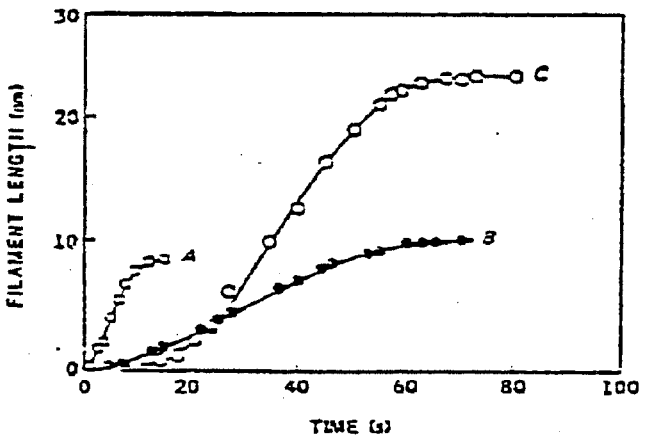

Figure 7-11. Growth-rate Curves for Filamentous Carbon from (a) Nickel-, (b) Iron-, and (c) Cobalt-catalyzed Decomposition of Acetylene

Reference: (30)

Table 7-3

Relationship Between Mobility Temperature of 10-nm Particles Supported on Graphite and Their Bulk Melting Points

Particle	Environment	Mobility temperature, K	Melting point, K	Ratio
Silver	O_2, H_2	623	1233	0.50
Gold	O_2	673	1336	0.50
Platinum	O_2	1123	2043	0.55
Palladium	O_2	1023	1825	0.56
Iridium	O_2	1348	2683	0.50
Rhodium	O_2	1182	2239	0.53
Iron	CO_2, CO	973	1908	0.54
Cobalt	C_2H_2	918	1768	0.52
Nickel	H_2, C_2H_2	913	1726	0.53
Molybdenum	C_2H_2	1453	2893	0.50
Calcium oxide	O_2	1493	2853	0.52
Barium oxide	O_2	1110	2196	0.50
Zinc oxide	O_2	1173	2248	0.52

Reference: (30)

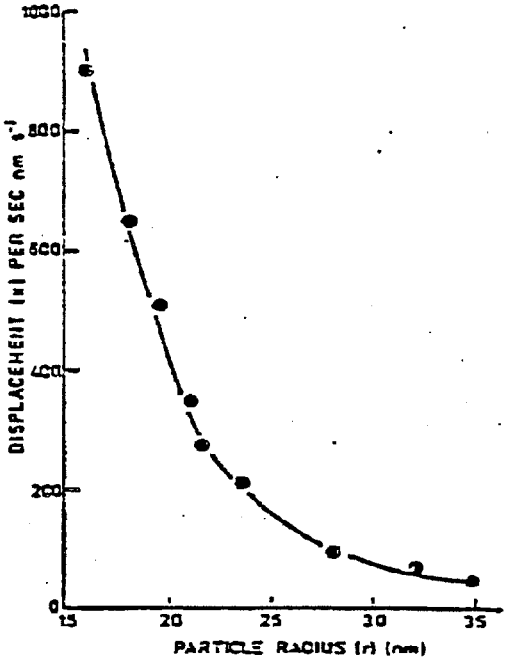

Figure 7-12. Variation of Particle Displacement Rate with Particle Radius for Silver Heated in 2.0 torr Hydrogen at 365°C

Reference: (30)

upward, and the upper size limit of particles exhibiting mobility increased. Particle growth was observed below the Tammann point, although the growth rate was much lower. This growth was attributed to atomic migration.

Figure 7-13 shows the variation of average Pd particle size with temperature in the presence of acetylene, ethylene, oxygen, and argon. In oxygen, the channeling activity of graphite substrate increases rapidly at 800°C, resulting in agglomeration.

CAEM is an important tool in catalysis research. Baker's techniques, as demonstrated in the preceding examples, may be applied to study carbon formation at the autothermal reforming inlet and catalyst sintering in high-temperature steam reforming.

Baker also studied Pt-and Ir-catalyzed gasification of graphite by means of CAEM (31). In the test, single-crystal graphite was coated with a monolayer of Pt, Ir, and Pt/Ir alloy in 80/20 atomic ratio. Hydrogen flow was maintained under a pressure of 1 torr. Under these conditions, the following results were observed:

For Pt on graphite:

- The Pt film nucleated at 500°C to form small particles of ~2.5 nm diameter. These particles grew in size to 25-35 nm in the 500-700°C range.

- As the temperature was raised to 755°C, particles not only ceased to grow but became lighter in appearance, suggesting that metal was being lost from those surfaces not in contact with graphite. During this process, no particle motion was evident.

- Increasing the temperature to 845°C resulted in renucleation of particles of 2.5-nm diameter at positions away from the original particles. After 10 min. at 845°C, these fresh particles grew to 10-25 nm.

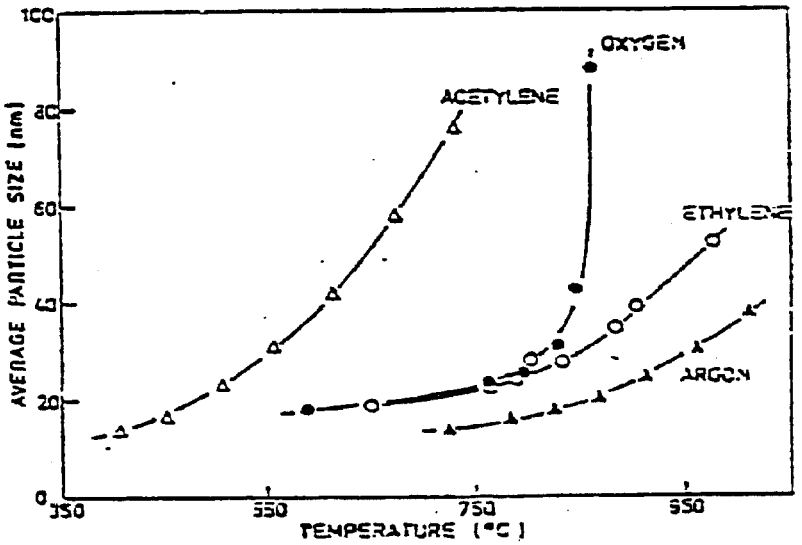

Figure 7-13. Variation of Palladium Average Particle Size with Temperature in Various Gaseous Environments (Graphite Support)

Reference: (30)

- At 1000°C, particles became active in gasification.

- Above 1150°C, the particles fragmented into two or more smaller entities. The fragmentary particles continued to create channels but at a slower rate than the parent particle.

For Ir on graphite:

- Ir deposited as a carbonyl complex nucleated at 750°C in sizes of 5-20 nm and continued to grow up to 950°C.

- At 965°C, the particles became smooth and wetted the graphite surface. Over the same period, the particles disappeared in a fashion similar to that described for Pt, leaving an array of lighter patches as the only evidence of the existence of Ir particles.

- At 1050°C, the particles became active in channeling.

- At 1170°C, channeling became vigorous.

- At 1230°C, particle splitting was common.

For Pt/Ir on graphite:

- At 605°C, the monolayer of Pt/Ir in an 80/20 atomic ratio collected into a stringy network that eventually nucleated into particles.

- At 850°C, faceted particles became spherical, and they started to disappear as in the single-metal cases.

- At 970°C, channeling started.

- At 1050°C, channeling became vigorous.

The above results clearly show that the addition of Ir to Pt changes the nucleation and the carbon gasification properties. This naturally leads to the question of what effect Ir-alloying will have on Pt as a steam reforming catalyst, especially for distillate reforming. To date, little is known about this application. On the other hand, the Pt-Ir catalyst, together with Pt-Re, is widely used in catalytic reforming of naphtha for gasoline production.

Electron microscopy in combination with energy dispersive spectroscopy, whether it is SEM-EDS or TEM/STEM-EDS, offers a powerful tool in catalysis research. However, the hardware involved is substantial and costly. Furthermore, it requires expertise in practically all phases of the operation, including peripheral areas such as sample preparation.

7.5 SUMMARY AND CONCLUSIONS

Introductory descriptions of ESCA, AES, SIMS, and SEM-EDS have been given with some examples of their applications. These should provide answers to questions regarding:

- Applicability to commercial or developing F-T catalysts
- Types of information obtainable.

The methods described are rather sophisticated and require expertise to operate and interpret the results. This aspect cannot be taken lightly, as optimal impact on catalyst development is possible only when expertise in catalysis is joined with analytical expertise.